Available online at www.sciencedirect.com
SCIENCE DIRECT®
Catalysis Today 86 (2003) 61–72
CATALYSIS TODAY
www.elsevier.com/locate/cattod

Tailoring of alumina surfaces as supports for NiMo sulfide catalysts in the ultra deep hydrodesulfurization of gas oil: case study of TiO_2-coated alumina prepared by chemical vapor deposition technique

Youssef Saih, Kohichi Segawa*

Department of Chemistry, Faculty of Science and Technology, 7-1 Kioi-cho, Chiyoda-ku, Tokyo 102-8554, Japan

Received 11 March 2003; received in revised form 27 May 2003; accepted 28 May 2003

Abstract

The present paper gives a detailed review of the different studies under investigation in our laboratory concerning the use of TiO_2 and TiO_2–Al_2O_3 composites prepared by chemical vapor deposition (CVD) as support for sulfide catalysts in the HDS of dibenzothiophene (DBT) derivatives. The supports investigated here are: TiO_2 (from Degussa, 50 m^2/g), Al_2O_3 (Nikki, 186 m^2/g) and TiO_2–Al_2O_3 supports prepared by CVD of $TiCl_4$ on alumina. Using several characterization techniques, we have demonstrated that the support composite presents a high dispersion of TiO_2 over γ-Al_2O_3 without forming precipitates up to ca. 11 wt.% loading. Moreover, the textural properties of the support composite are comparable to those of alumina. XPS investigations of Mo and NiMo catalysts supported on the different carriers show that Mo-oxide species exhibit a higher degree of sulfidation on the surface of TiO_2 and TiO_2–Al_2O_3 than on alumina. The HDS tests of 4,6-DMDBT under mild operating conditions (573 K, 3 MPa) show that sulfide catalysts supported on the composite support (ca. 11 wt.%) are more active than those supported on to TiO_2 or Al_2O_3. This higher HDS catalytic activity is attributed to the promotion of the hydrodesulfurization pathway, whereby the pre-hydrogenation of one of the aromatic rings adjacent to the thiophenic one may reduce the steric hindrance caused by the two methyl groups adjacent to the sulfur atom during the C–S bond cleavage.

Keywords: TiO_2–Al_2O_3; Chemical vapor deposition; Hydrodesulfurization; XPS; Methyl-DBT derivatives

1. Introduction

Recently, there is a renewed interest in hydrodesulfurization (HDS) of gas oil because of new and more severe environmental regulations that will take effect in several industrialized countries in the near future. Indeed, in Japan and the E.U., e.g., the allowed sulfur content of gas oil will be reduced from 500 to 50 ppm in 2005, whereas in the USA it will be lowered to 15 ppm in 2006. Furthermore, there are plans to decrease the sulfur level of gas oil to very low content (less then 10 ppm) by the end of the current decade. To meet such very stringent environmental regulations, the hydrodesulfurization of crude oil in refineries under higher conditions of pressure and temperature (ultra deep hydrodesulfurization) seems to be for the moment the only method available for diesel manufacturing companies. However, due to

* Corresponding author. Tel.: +81-3-3238-3452; fax: +81-3-3238-4350.
E-mail address: k-segawa@sophia.ac.jp (K. Segawa).

0920-5861/$ – see front matter
doi:10.1016/S0920-5861(03)00404-8

the product quality specifications and also for safety reasons there are currently limits beyond which the temperature and pressure can be increased during the hydrodesulfurization process. Therefore, great effort will have to be devoted to the improvement of the refinement processes and to the design of a new family of highly active HDS catalysts.

For several decades, CoMo and NiMo/alumina have been used in industrial refining plants as HDS catalysts. Meanwhile, it has been reported by several authors that variation of the support influences the electronic and catalytic properties of supported NiMo and CoMo sulfide catalysts [1]. This may mean that a further increase in the HDS activity of supported sulfide catalysts can be achieved by changing the support. One of the most interesting carriers that is attracting increasing attention is titania. Although TiO_2 has a small surface area (50–70 m^2/g) compared to that of alumina, Mo/TiO_2 catalysts exhibit three to four times higher HDS activity (per mole Mo) than Mo/Al_2O_3 [2,3]. Several investigators have attempted to understand such outstanding increase in the HDS catalytic activity using several experimental techniques [4–16]. It was concluded that Mo catalysts supported on TiO_2 are uniformly dispersed on the support surface and are better sulfided than on alumina. Moreover, it was recently suggested that the role of titania is not only to act as a conventional support but also as an electronic promoter [17,18]. A further increase in the HDS activity of Mo/TiO_2 can be achieved if one can overcome the different deficiencies related to the small surface area of titania and the low thermal stability of the active anatase form. Consequently, several researchers used the thermal stability of alumina to sustain the crystal structure of titania in TiO_2–Al_2O_3 mixed oxides [19–38]. Meanwhile, within our research team we have already demonstrated that coating the γ-Al_2O_3 surface with titania using a chemical vapor deposition technique (CVD) may constitute an interesting strategy to overcome the titania disadvantages [39–42]. Furthermore, it was recently demonstrated that the use of titania with a relatively higher specific surface area and a good thermal stability leads to an increase in the specific HDS catalytic activity of Mo/TiO_2 catalysts [43–45].

To lower the sulfur content of diesel fuel below the 500 ppm level one will have to deal with the most refractory S-containing compounds still present in gas oil. Such species are currently known to be the alkyl-dibenzothiophenes (alkyl-DBT) (Fig. 12) especially those substituted in the 4 and 6 positions of the DBT skeleton such as 4,6-dimethyldibenzothiophene (4,6-DMDBT). Indeed, since the last decade of the last century, a great part of the scientific research currently done in all the laboratories concerning the ultra deep HDS is focused on the study and understanding of the chemistry of the DBT derivatives. Recently, several review papers related to the chemistry of these species have been published [46,47].

The present paper reviews in detail the different studies under investigation in our laboratory concerning the use of TiO_2 and TiO_2-coated alumina prepared by CVD as supports for Mo and NiMo sulfide catalysts in the HDS of alkyl-DBT derivatives.

2. TiO_2–Al_2O_3 supports prepared by CVD

The different supports investigated here are as follows: TiO_2 (P-25 from Degussa, 50 m^2/g), γ-Al_2O_3 provided by NIKKI (N611-N, 186 m^2/g), and TiO_2-coated alumina supports prepared by CVD.

The TiO_2–Al_2O_3 composites are prepared by chemical vapor deposition technique using $TiCl_4$ as a precursor. In a quartz tubular reactor, 2 g of γ-Al_2O_3 are pretreated at 773 K under oxygen flow (25 cm^3/min) for 2 h; after that the substrate is exposed to $TiCl_4$ (WAKO) vapor/N_2 (P_{TiCl_4} = 0.43 kPa) at 473 K. In order to prepare supports with different TiO_2 loading, we varied the deposition time from 0.5 to 20 h. The different samples are then hydrolyzed under H_2O/N_2 gas stream (P_{H_2O} = 2.30 kPa) at 473 K for 2 h. Finally, the solids are calcined at 773 K under O_2 flow for 2 h.

The TiO_2–Al_2O_3 composites prepared by CVD are characterized using several experimental techniques, as described below. The TiO_2 overall content is determined from X-ray fluorescence (XRF) measurements performed on a SXF-1200 analyzer from Shimadzu. The results obtained for the different TiO_2–Al_2O_3 composites prepared at different decomposition times are given in Table 1. XRF studies clearly reveal an increase of the TiO_2 loading with increasing the deposition time.

FT-IR spectroscopy is used to detect changes of the vibrational bands of hydroxyl groups on the alumina surface after deposition of TiO_2. IR measurements

Table 1
Specific surface area and pore volume of γ-Al_2O_3, TiO_2 and composite TiO_2–Al_2O_3 support loaded with different amounts of titania[a]

Deposition time (h)	TiO_2 (wt.%)	Specific surface area (m^2/g)	Pore volume (cm^3/g)
0	–	186	0.44
0.5	2.53	182 (187)	0.42
4	4.86	177 (186)	0.41
8	6.64	174 (186)	0.40
12	8.94	168 (185)	0.36
16	11.15	162 (183)	0.37
20	13.69	154 (179)	0.35

[a] Values in parentheses correspond to the specific surface area calculated for 1 g of alumina.

are taken at room temperature on a Shimadzu FTIR 8200PC, in the range from 3600 to 3900 cm^{-1}. Before data collection, the samples were evacuated in situ at 773 K for 2 h. The IR spectra of γ-alumina and TiO_2–Al_2O_3 composite supports with different loadings of titania are displayed in Fig. 1.

Before CVD treatment, we observe the presence of bands at 3762, 3723 and 3680 cm^{-1} corresponding to hydroxyl stretching vibrations of Al–OH groups present on the alumina surface. These bands are rather broad, due to the fact that the alumina carrier is a poorly crystalline material. Increasing of the TiO_2 loading up to ca. 11 wt.% leads to a strong decrease of the integrated intensities of all observed vibrational bands. This implies the substitution of Al–OH groups on the surface of γ-Al_2O_3 by Al–O–Ti bridges during the CVD process.

In order to get more insight into the dispersion state of TiO_2 over γ-Al_2O_3, we investigated the textural properties of the different TiO_2–Al_2O_3 supports prepared by CVD using nitrogen adsorption measurements at 77 K. Specific surface areas and pore volumes of γ-Al_2O_3 and TiO_2–Al_2O_3 composites containing different amounts of titania, are depicted in Table 1. Increasing the TiO_2 loading up to ca. 13.7 wt.% leads to a decrease of the specific surface area of the TiO_2–Al_2O_3 supports from 186 m^2/g for pure alumina to 154 m^2/g. However, the specific surface area calculated for 1 g of alumina is not significantly affected. It is noteworthy that, even at 13.7 wt.% TiO_2 loading, the surface area of the TiO_2–Al_2O_3 composite is still three times larger than the specific surface area of the commercially available pure TiO_2 (ca. 50 m^2/g).

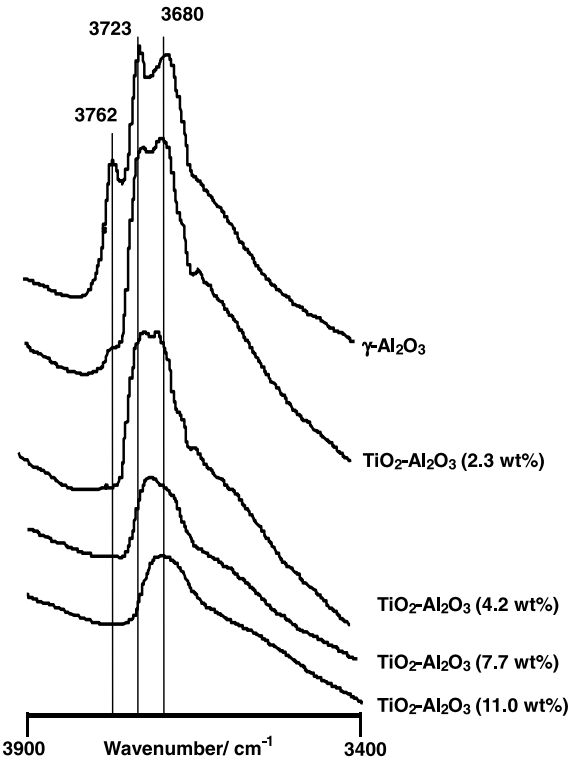

Fig. 1. IR spectra of γ-Al_2O_3 and composite TiO_2–Al_2O_3 supports with different TiO_2 loadings. The values between parentheses represent the TiO_2 loadings.

Consequently, a large specific surface area and a large pore volume are still preserved while coating the alumina support with TiO_2 using the CVD technique.

Fig. 2 shows the pore size distribution obtained for Al_2O_3, TiO_2 (Degussa, P-25) and TiO_2–Al_2O_3 composite supports.

It can be seen that pure TiO_2 possesses no pore system. Deposition of titania on alumina leads to the formation of a composite support with a pore size distribution similar to that of the substrate. Meanwhile, the pore volume is only slightly decreased. Consequently, the resulting TiO_2–Al_2O_3 composite remains mesoporous, with a more or less monomodal pore size distribution and an average pore radius of about 3.8 nm.

Bulk and surface composition of TiO_2–Al_2O_3 supports prepared by CVD as determined by XRF and X-ray photoelectron spectroscopy (XPS), respectively, are depicted in Fig. 3. The XPS measurements were performed on a Surface Science laboratory SSX-100

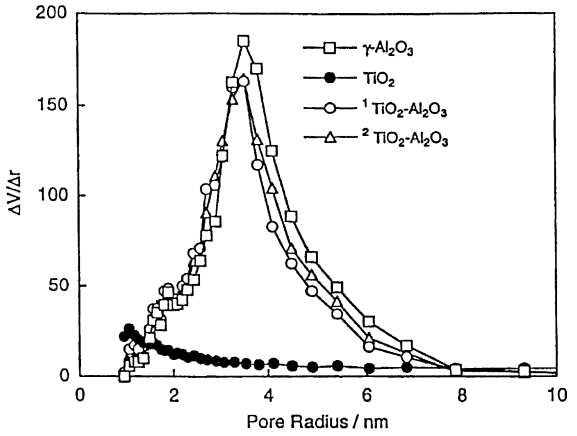

Fig. 2. Pore size distribution of different supports. (1) 6.80 wt.% TiO_2; (2) 11.20 wt.% TiO_2.

spectrometer, using monochromized Al Kα radiation (1486.6 eV); the C (1s) binding energy (284.8 eV) was taken as a reference.

The increase of the total TiO_2 loading determined by XRF leads to a linear increase of TiO_2 amount on the Al_2O_3 surface. Moreover, the surface Ti/Al atomic ratio is higher than the bulk Ti/Al within the TiO_2 loading investigated here (Fig. 3). Thus, we can conclude that the incorporation of significant amounts of titanium into the γ-Al_2O_3 matrix can be excluded within the sensitivity of the investigation methods used here.

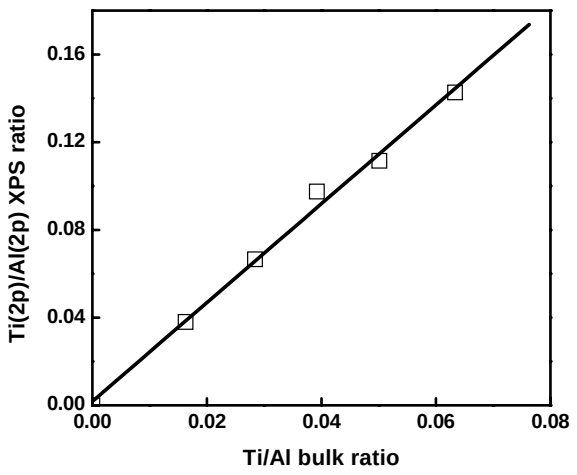

Fig. 3. Bulk and surface composition of TiO_2–Al_2O_3 supports prepared by CVD.

Consequently, in the case of TiO_2–Al_2O_3 composites prepared by CVD, titania mainly covers the surface of γ-Al_2O_3 support without forming precipitations. Moreover, the textural properties of the composite support are very similar to those of alumina. The IR investigations support such an assumption, even though the vibrational bands of Al–OH groups are not completely eliminated at loadings up to 11 wt.% TiO_2. This might be due to the fact that the alumina surface is not completely covered. In fact, assuming that titania forms a monolayer, the surface of alumina would be completely covered only at 15 wt.% TiO_2. Furthermore, it is known that in the bulk phase of poorly crystalline alumina there are Al–OH groups present even after calcination. These hydroxyl groups cannot be substituted by Al–O–Ti bridges, and the corresponding vibrational bands in the IR spectra remain unchanged. Nevertheless, higher loadings of TiO_2 may lead to a more complete elimination of hydroxyl bands on the alumina surface. The comparison of the surface composition and the total amount of TiO_2 (Fig. 3) unambiguously revealed that titania is highly dispersed on the alumina surface. The TiO_2 loading of the composite support used for the next investigations is ca. 11 wt.%, which corresponds to an almost complete coating of alumina surface.

3. XPS studies

3.1. Mo catalysts

Molybdenum is deposited on the supports by impregnation at 323 K using ammonium heptamolybdate solution with the required concentration. After impregnation, all the samples are dried at 373 K for 12 h, then calcined at 773 K for 10 h.

It is widely accepted that supported Mo-species are present on the surface of hydrodesulfurization catalysts in a highly dispersed state. Therefore, the use of conventional bulk characterization techniques cannot help in determining the chemical state of Mo catalysts supported onto TiO_2, TiO_2–Al_2O_3 and Al_2O_3. XPS can provide interesting information concerning the state of highly dispersed catalysts. In the following section we describe the states of supported Mo-species before and after sulfurization using XPS.

3.1.1. Oxidic state

The Mo(3d) XPS spectra for calcined catalysts (6 wt.% MoO_3 nominal loading) and crystalline MoO_3 are illustrated in Fig. 4 (spectra A–D). For all the catalysts, the Mo(3d) XPS peaks show doublets similar to that of MoO_3, indicating that supported Mo-species are present in Mo(VI) state. However, the peaks obtained for Mo/Al_2O_3 are much broader than those obtained for MoO_3, Mo/TiO_2 and Mo/TiO_2–Al_2O_3. Moreover, the FWHM values (not shown here) increase in the following order: $Mo/TiO_2 < Mo/TiO_2$–$Al_2O_3 < Mo/Al_2O_3$. Earlier, it has been reported that a strong interaction between molybdena and alumina favors the presence of more than one type of Mo(VI) species on the alumina surface [48,49]. Therefore, the broadening of the Mo(3d) XPS peaks of Mo/Al_2O_3 can be attributed to the strong interaction between Mo and the alumina. Meanwhile, the interaction between Mo-species and titania seems to be lower than with alumina, leading to the formation of a more uniform distribution of Mo-oxidic species and well-resolved Mo(3d) XPS doublets [40]. For the same reasons, we can conclude that the interaction between Mo-species and the composite support is lower than with alumina, yet higher than with titania. Accordingly, covering the surface of alumina with titania lowers the interaction between Mo-oxidic species and Al_2O_3.

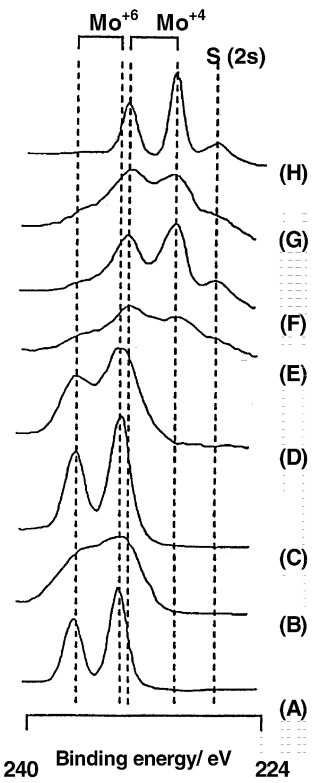

Fig. 4. Mo(3d) XPS spectra of the calcined catalysts (B, C, D), the sulfided materials (E, F, G), crystalline MoS_2 (H) and MoO_3 (A). Mo/Al_2O_3 (B, E), Mo/TiO_2 (C, F), Mo/TiO_2–Al_2O_3 (D, G). Mo nominal loading: 6.0 wt.% MoO_3.

3.1.2. Sulfidic state

The sulfidation properties of Mo/Al_2O_3, Mo/TiO_2 and Mo/TiO_2–Al_2O_3 catalysts (6 wt.% MoO_3) were investigated by XPS. The samples were sulfided at 673 K for 2 h in a H_2S/H_2 (5 vol.% H_2S) mixture.

After sulfurization, the maxima due to Mo(VI) species have strongly decreased (Fig. 4, spectra E–H). The binding energies for crystalline MoS_2 are 233.0 eV ($3d_{3/2}$) and 229.9 eV ($3d_{5/2}$). The spectra of sulfided MoO_3 on the different supports can also be assigned to MoS_2 species, whereas Mo(VI) species are still present. As already obtained for the calcined materials, sulfided Mo/Al_2O_3 reveal broader Mo(3d) XPS peaks than MoS_2, Mo/TiO_2 and Mo/TiO_2–Al_2O_3 catalysts. This might be explained by the reasons mentioned above. The Mo($3d_{5/2}$) binding energies of the sulfided catalysts increase as follows: $Mo/Al_2O_3 < Mo/TiO_2$–$Al_2O_3 = Mo/TiO_2$.

The effect of Mo loading (0–30 wt.% MoO_3) on the sulfidation properties of molybdenum catalysts supported on TiO_2, Al_2O_3 and TiO_2–Al_2O_3 is described below. The fraction of the MoS_2 present on the catalyst surface is estimated from the Mo(IV)/Mo(IV) + Mo(VI) area ratio of the corresponding XPS peaks in the 3d region (Fig. 5).

Fig. 5 shows that the fraction of MoS_2 present on alumina increases with increasing the Mo loading up to ca. 15 wt.% MoO_3; then it leveled off. At low molybdenum loadings, the relatively low sulfidation of Mo-species supported on alumina can be attributed to the higher interaction between alumina and molybdenum oxidic species, as reported above (Fig. 4). Besides, it was already reported by Li and Hercules that, at low Mo loadings, isolated molybdenum species in tetrahedral configuration (Mo_{tet}) cannot be reduced to Mo(IV) even at temperatures as high as 773 K [50]. The same authors reported also that the reducibility of Mo-species supported on alumina increases with

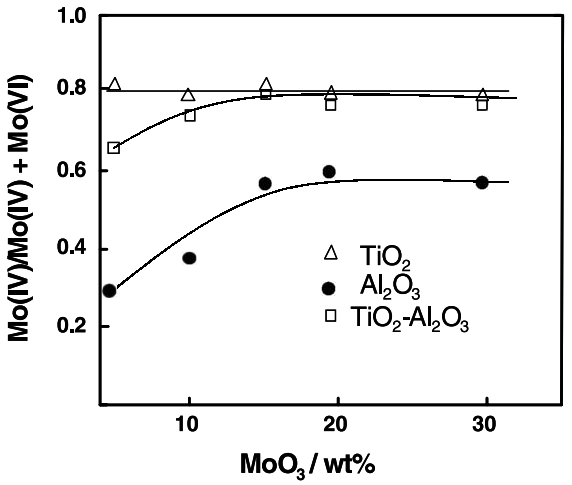

Fig. 5. Sulfidation of Mo-species supported on different carriers vs. Mo loading, as determined by XPS.

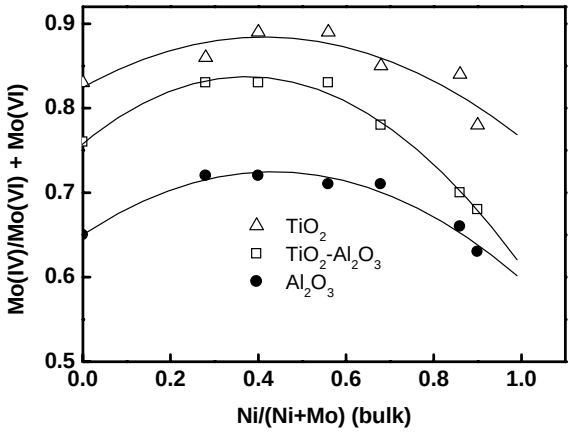

Fig. 6. Fraction of MoS_2 supported on different carriers vs. Ni/(Ni + Mo) bulk atomic ratio.

molybdenum loading. However, for Mo/TiO_2 catalysts the ratio Mo(IV)/Mo(IV) + Mo(VI) is relatively higher than that observed in the case of alumina. Moreover, this ratio is constant within the Mo range investigated here and is equal to ca. 80%. This means that Mo-species supported onto titania are highly sulfided than on alumina. The relatively higher sulfidation of Mo-species supported on TiO_2 compared to those supported over alumina has been also reported by Okamoto et al. [9]. Mo/TiO_2–Al_2O_3 catalysts show the same behavior as Mo/Al_2O_3; however, the fraction of MoS_2 on the composite support is higher than on alumina and approaches that of Mo/TiO_2 with increasing Mo loading.

3.2. NiMo catalysts

NiMo catalysts are prepared by successive impregnation (Mo first) using ammonium heptamolybdate and nickel nitrate solutions with the adequate concentrations. The solids were then treated as reported above for Mo catalysts. The Ni- and NiMo-supported catalysts were also sulfided at 673 K as reported above.

The different features of Mo XPS spectra of NiMo sulfide catalysts (BE and FWHM) are similar to those of MoS_2. Consequently, the structure of molybdenum species in NiMo sulfide catalysts supported on the different carriers investigated here is similar to that of MoS_2.

Fig. 6 represents the variation of the amount of MoS_2 on the catalyst surface versus the Ni/(Ni + Mo) bulk atomic ratio. The total loading of nickel and molybdenum (NiO + MoO_3) was kept constant and equal to 20 wt.%.

We can see that the Mo(IV)/(Mo(IV) + Mo(VI) ratio increases with Ni/(Ni + Mo) bulk atomic ratio up to 0.5 and then it decreases, for all the carriers investigated here. This can be considered to be one of the promoting aspects of nickel. For the moment, such an increase in the molybdenum sulfidation degree could not be explained. Besides, it should be noted that the reducibility of molybdenum species from oxidic to sulfidic state decreases in the following order: Al_2O_3 < TiO_2–Al_2O_3 < TiO_2, as was observed above for unpromoted Mo catalysts (Fig. 5).

Consequently, under the present sulfidation conditions, Mo-species supported on both TiO_2 and TiO_2–Al_2O_3 catalysts are highly sulfided, leading to the formation of a MoS_2-like structure. However, on alumina the sulfidation of Mo is rather difficult, due to the relatively higher interaction of Mo-species with alumina. For NiMo catalysts, sulfidation of Mo increases in the following order: $NiMo/Al_2O_3$ < $NiMo/TiO_2$–Al_2O_3 < $NiMo/TiO_2$. Moreover, addition of Ni to Mo catalysts seems to improve the sulfidability of Mo, which can be considered to be one of the promoting aspects of Ni.

4. HDS reaction of dibenzothiophene derivatives

DBT derivatives are the most refractory S-containing compounds present in gas oil, especially those substituted in the 4 and 6 position of the DBT skeleton (see Fig. 12). Currently, it is widely accepted that the HDS of alkyl-DBT derivatives proceeds through two parallel reaction routes as shown below in the case of 4,6-DMDBT. The first pathway is direct extraction of the sulfur atom (hydrogenolysis). The second pathway is pre-hydrogenation of one aromatic ring, followed by sulfur removal (hydrodesulfurization).

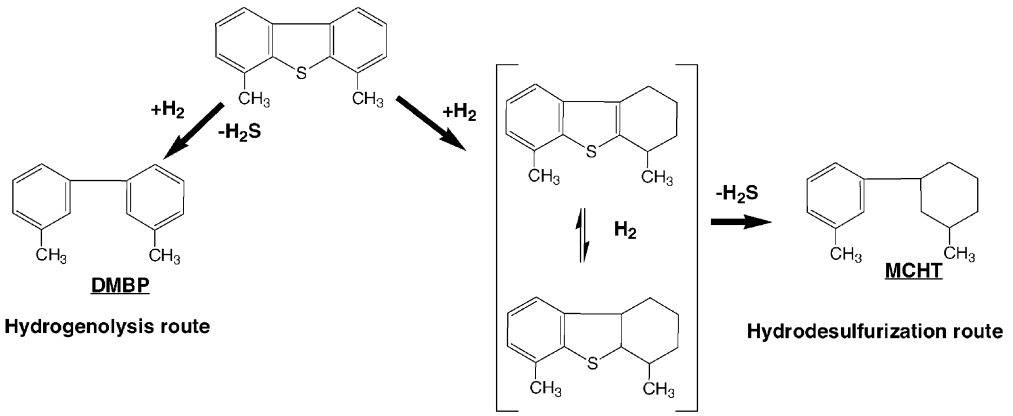

Two theories have been put forward to explain the low reactivity of these species. The first hypothesis suggests that the transformation of these species is limited by the adsorption step, since the presence of methyl groups in the sulfur neighborhood may alter the adsorption of the substrate through the sulfur atom (end-on adsorption) and thus lead to a decrease in their intrinsic reactivity [51–54]. The second theory suggests that all DBTs derivatives, including both 4-MDBT and 4,6-DMDBT species, are adsorbed on the catalyst surface through the aromatic ring adjacent to the thiophenic one (side-on adsorption). In this case, the low reactivity of the hindered species is attributed to the steric hindrance caused by the alkyl groups adjacent to the sulfur atom during the C–S bond cleavage [55–58].

Recently, Kabe and coworkers reported a kinetic study of DBT derivatives HDS over three different $CoMo/Al_2O_3$ industrial catalysts under mild operating conditions (363–613 K, 5 MPa) [59]. The authors reported that the 4-MDBT and 4,6-DMDBT substrates exhibit higher heats of adsorption compared to that of DBT. They conclude that the methyl-substituted DBT species are more easily adsorbed on the catalyst surface than DBT is. Indeed, they suggested that DBT, 4-MDBT and 4,6-DMDBT are side-on adsorbed on the catalyst surface and thus the adsorption step cannot be considered as the rate-limiting step for the hindered DBT HDS process. The relatively higher yield of cyclohexylbenzene (CHB) derivatives observed by the authors during the HDS of hindered DBT was attributed to the fact that the partial or total pre-hydrogenation of one of the aromatic rings adjacent to the thiophenic one forces the methyl groups out of the sulfur ring system (puckering), leading to a decrease of the steric hindrance during the subsequent C–S bond breakage.

To elucidate the influence of the position of the methyl groups on the conversion rate in a mixture of methyl-DBT derivatives, we investigated the HDS of a mixture A of DBT, 4-MDBT, and 4,6-DMDBT (molar ratio: 1/1/1) over Mo/Al_2O_3 catalyst (6 wt.% MoO_3). For comparison, the HDS of a mixture B of DBT, 2-MDBT and 2,8-DMDBT (molar ratio: 1/1/1) has been performed under the same reaction conditions. The HDS reaction is carried out in a fixed bed high-pressure flow reactor, consisting of a 0.5 in. stainless steel tube packed with 250 mg catalyst mixed with quartz sand. Before the reaction, the catalysts were calcined at 773 K for 5 h under oxygen stream and pre-sulfided with a mixture of H_2S (5%) and H_2 for 2 h at 673 K under atmospheric pressure. After the H_2S excess was purged by nitrogen stream at 673 K for 0.5 h, H_2 and the reaction mixture are supplied to the reactor.

Table 2
Effect of methyl substitution in DBT skeleton on HDS catalytic activity of Mo/Al_2O_3 catalyst[a]

	DBT	2-MDBT	4-MDBT	2,8-DMDBT	4,6-DMDBT
Mixture A					
Relative activity	1.00		0.43		0.17
Mixture B					
Relative activity	1.00	1.50		1.97	

[a] Reaction conditions: reaction pressure 3 MPa, reaction temperature 573 K, LHSV 12–16 h^{-1}, H_2 flow rate 200 ml min^{-1}. The molar ratio of DBT derivatives in mixtures A and B is 1/1/1.

All reaction mixtures used in this study were diluted in *n*-dodecane. The reaction temperature is 573 K (H_2 pressure: 3 MPa, H_2 flow rate: 0.2 dm^3/min, LHSV: 12–16 h^{-1}). The liquid products collected from a gas–liquid separator were analyzed by GC (Hitachi G-3000) and GC–MS (GC: Hewlett Packard 5890 series II, MS: Nihondenshi JMS-SX 102A). The activity is estimated by the conversion of the DBT derivatives and by the ratio of the products after reaching steady state. The major products detected are unreacted DBTs species, cyclohexylbenzene (CHBs) and biphenyl (BPs) derivatives.

The results of methyl-DBTs hydrodesulfurization activity over Mo/Al_2O_3 catalyst are depicted in Table 2. The HDS activity of DBT was taken as a reference. As expected, the conversion for the different compounds increases as follows: DBT > 4-MDBT > 4,6-DMDBT. For the second mixture B, the HDS reactivity increases in the following order: 2,8-DMDBT > 2-MDBT > DBT. Consequently, the 2,8-DMDBT species is the most reactive one among the series investigated here. This was also reported earlier by Kilanowski et al. [60]. Therefore, isomerization of the alkyl groups on molecules such as 4,6-DMDBT to positions that do not sterically interfere with the catalytic active sites during the HDS process will lead to an increase in the HDS activity. This was recently proven by several authors using a combination of conventional HDS catalysts and acidic compounds such as zeolites [61,62].

In order to get more insight into the influence of the support on the methyl-substituted DBT derivatives reaction pathways, we carried out the HDS of the mixture A at different contact times. The catalysts used were Mo/TiO_2, Mo/Al_2O_3 and Mo/TiO_2–Al_2O_3 with a 6 wt.% MoO_3 loading. The results are illustrated in Fig. 7. For all the catalysts, we observe an increase of both conversion and CHBs selectivity while increasing the contact time. Comparing the three sulfur compounds, we can see that the CHBs/BPs ratio increases in the following order: DBT < 4-MDBT < 4,6-DMDBT. This implies that the HDS of 4,6-DMDBT proceeds principally through the hydrodesulfurization pathway, leading to relatively higher CHBs/BPs ratios.

In the cases of DBT and 4-MDBT, the effect of support on the HDS reaction routes is negligible. For 4,6-DMDBT, however, the CHBs/BPs derivatives ratio is relatively higher for Mo/TiO_2 and Mo/TiO_2–Al_2O_3 catalysts compared to that of Mo/Al_2O_3.

The HDS of 4,6-DMDBT and the product selectivity were studied on Mo/TiO_2, Mo/Al_2O_3 and Mo/

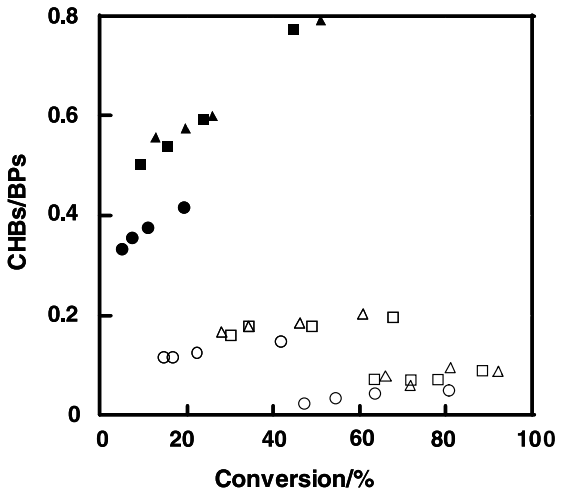

Fig. 7. CHBs/BPs ratio as a function of conversion of an equi-molar mixture of DBT derivatives (DBT, 4-MDBT and 4,6-DMDBT) at 573 K and 3 MPa. Open symbols represent 4-DMDBT, closed symbols represent 4,6-DMDBT, dashed symbols represent DBT; Mo/TiO_2–Al_2O_3 (squares), Mo/TiO_2 (triangles), Mo/Al_2O_3 (circles). The MoO_3 loading of the catalysts is 6 wt.%.

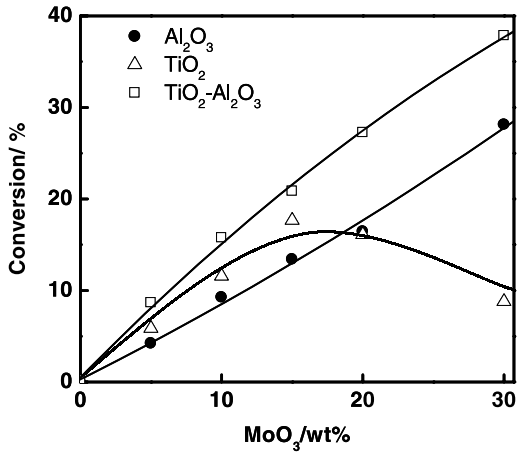

Fig. 8. HDS activities for 4,6-DMDBT over Mo/TiO_2–Al_2O_3 (11 wt.% TiO_2), Mo/TiO_2 and Mo/Al_2O_3 catalysts as a function of Mo loadings. Operating conditions: $T = 573$ K, $P = 3$ MPa, LHSV = 12–16 h^{-1} and H_2 flow rate = 200 cm^3/min.

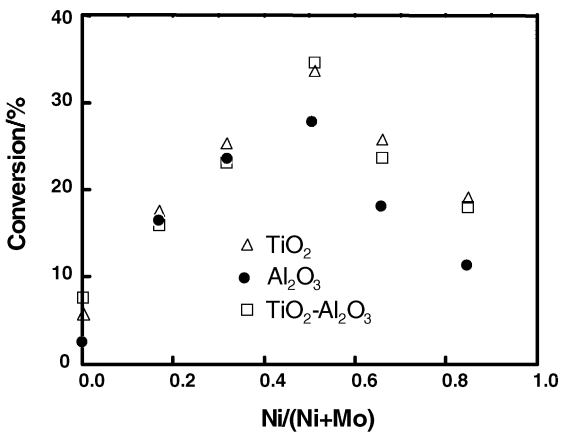

Fig. 10. Conversion of 4,6-DMDBT vs. Ni/(Ni + Mo) bulk atomic ratio for NiMo sulfide catalysts supported on different carriers. Operating conditions: $T = 573$ K, $P = 3$ MPa, LHSV = 12–16 h^{-1} and H_2 flow rate = 200 cm^3/min.

TiO_2–Al_2O_3 catalysts with different molybdenum loadings (Mo: 3–30 wt.% MoO_3). The results are depicted in Figs. 8 and 9. We can see that the 4,6-DMDBT HDS catalytic activity increases for both Mo/Al_2O_3 and Mo/TiO_2–Al_2O_3 catalysts with Mo content. For Mo/TiO_2 catalysts, however, the HDS activity shows a maximum around 15 wt.% MoO_3 loading. Furthermore, Mo/TiO_2–Al_2O_3 catalysts exhibit the highest catalytic activity. The methylcyclohexyltoluene (MCHT) selectivity increases with the molybdenum loading for all the catalysts (Fig. 9). The MCHT selectivity over Mo/TiO_2 and Mo/TiO_2–Al_2O_3 catalysts is higher than that observed in the case of Mo/Al_2O_3 catalysts. Accordingly, the hydrodesulfurization pathway seems to be promoted for molybdenum catalysts supported on TiO_2 and on TiO_2–Al_2O_3 supports.

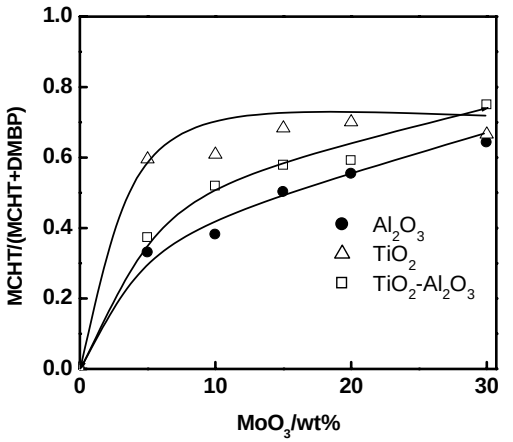

Fig. 9. Product selectivity for 4,6-DMDBT HDS reaction over Mo/TiO_2–Al_2O_3 (11 wt.% TiO_2), Mo/TiO_2 and Mo/Al_2O_3 catalysts. Operating conditions: $T = 573$ K, $P = 3$ MPa, LHSV = 12–16 h^{-1} and H_2 flow rate = 200 cm^3/min.

The 4,6-DMDBT HDS activities over NiMo sulfide catalysts supported on Al_2O_3, TiO_2 and TiO_2–Al_2O_3 at 573 K and 3 MPa are depicted in Fig. 10. The total loading of nickel and molybdenum ($NiO+MoO_3$) was kept constant and equal to 10 wt.%. For all the catalysts investigated here, a maximum in the HDS catalytic activity is observed for a $Ni/(Ni + Mo)$ ratio equal to 0.5. The $NiMo/Al_2O_3$ catalyst exhibits the lowest catalytic activity. Meanwhile, $NiMo/TiO_2$–Al_2O_3 and $NiMo/TiO_2$ catalysts exhibit almost the same catalytic activity. Nevertheless, we expect a relatively increase in the HDS catalytic activity of $NiMo/TiO_2$–Al_2O_3 compared to that of $NiMo/TiO_2$ for higher Metal loadings (e.g. 20 wt.%). The MCHT/(MCHT + DMBP) ratios observed for all the catalysts investigated here present a maximum for Ni/(Ni + Mo) ratio 0.5 (Fig. 11). It seems, however, that the contribution of the hydrodesulfurization pathway to the

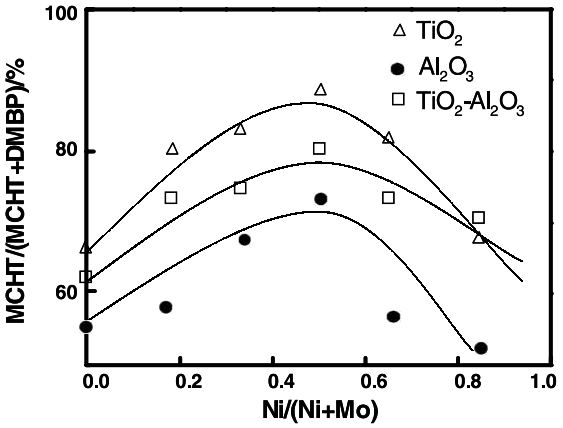

Fig. 11. Product selectivity for the conversion of 4,6-DMDBT vs. Ni/(Ni + Mo) bulk atomic ratio over NiMo sulfide catalysts supported on different carriers. Operating conditions: $T = 573\,K$, $P = 3\,MPa$, LHSV = 12–16 h^{-1} and H_2 flow rate = 200 cm^3/min.

overall desulfurization of 4,6-DMDBT is relatively important for $NiMo/TiO_2$ and $NiMo/TiO_2$–Al_2O_3 catalysts.

5. Conclusion

Consequently, the desulfurization of 4,6-DMDBT, one of the most refractory S-containing compounds that is present in considerable amounts in gas oil, seems to proceed principally through the hydrodesulfurization route (Fig. 7). In fact, the pre-hydrogenation of one of the aromatic rings adjacent to the thiophenic one decreases the steric hindrance caused by the two methyl groups. A further increase in the reactivity of 4,6-DMDBT can be achieved by using catalysts with both higher hydrogenation and higher desulfurization activity. The use of TiO_2 as a support seems to promote the hydrogenation activity of sulfide catalysts and thus increases the over-all desulfurization rate of 4,6-DMDBT, especially for relatively lower metal loadings. However, a further increase in the amount of Mo leads to a decrease in the HDS catalytic activity of Mo/TiO_2. This can be attributed to the low surface area of titania. For this reason, we opted for the use of TiO_2–Al_2O_3 composite prepared by CVD as a support for Mo and NiMo sulfide catalysts. In fact, TiO_2-coated Al_2O_3 supports exhibit textural properties similar to those of alumina and surface properties similar to those of titania. Moreover, Mo-oxide species supported on the composite carrier are better sulfided than on alumina and probably more dispersed than on titania. This leads to an increase of the number of HDS active centers known to be coordinatively unsaturated sites, as shown in Scheme 1. For these reasons the Mo/TiO_2–Al_2O_3 catalysts exhibit the highest activity for the HDS of 4,6-DMDBT.

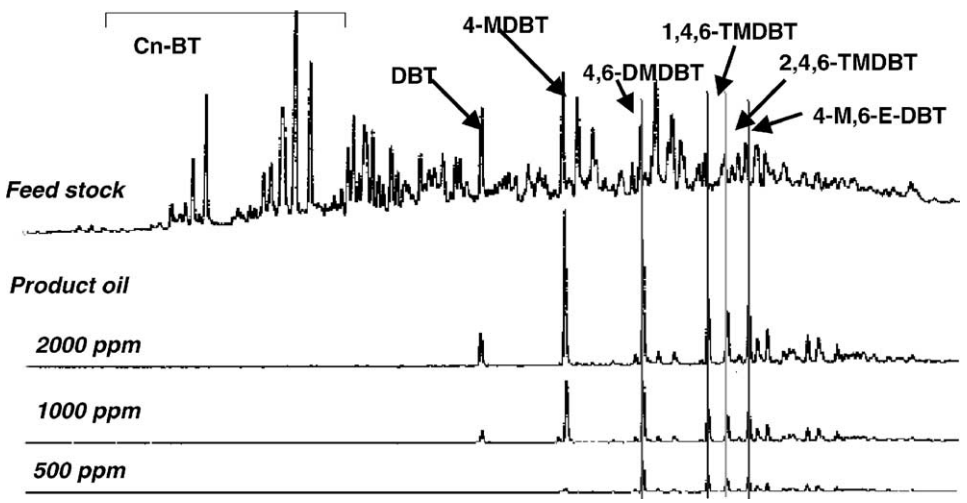

Fig. 12. Chromatogram showing S-containing compounds present in Arabian distillate oil after HDS at different sulfur levels. (M) methyl; (E) ethyl.

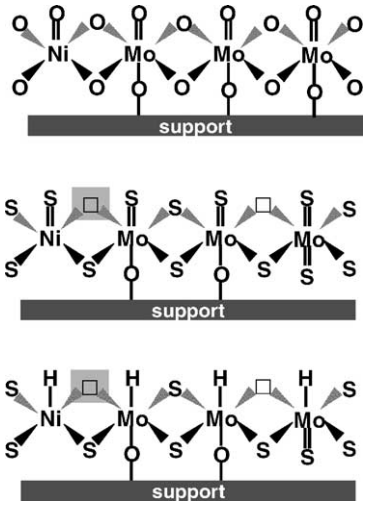

Scheme 1. Model for NiMo supported sulfide catalysts. (□) vacancy.

Acknowledgements

This work has been supported by the New Energy and Industrial Technology Development Organization (NEDO) under a subsidy of the Japanese Ministry of Economy, Trade and Industry (METI).

References

[1] H. Topsøe, B.S. Clausen, F.E. Massoth, in: J.R. Anderson, M. Boudart (Eds.), Hydrotreating Catalysis Science and Technology, vol. 11, Springer, New York, 1996, pp. 65–69, and references therein.
[2] K. Y. S. Ng, E. Gulari, J. Catal. 92 (1985) 340.
[3] K. Y. S. Ng, E. Gulari, J. Catal. 95 (1985) 33.
[4] S. Matsuda, A. Kato, Appl. Catal. 8 (1983) 149.
[5] J. Ramirez, S. Fuentes, G. Diaz, M. Vrinat, M. Breysse, M. Lacroix, Appl. Catal. 52 (1989) 211.
[6] A. Fernandez, J. Leurer, A. R. Gonzales-Elipe, G. Munuera, H. Knozinger, J. Catal. 120 (1988) 489.
[7] Y. Masuyama, Y. Tomatsu, K. Ishida, Y. Kurusu, K. Segawa, J. Catal. 114 (1988) 347.
[8] D. S. Kim, Y. Kurusu, I. E. Washs, F. D. Hardcastle, K. Segawa, J. Catal. 120 (1989) 325.
[9] Y. Okamoto, A. Maezawa, T. Imanaka, J. Catal. 120 (1989) 29.
[10] K. Segawa, T. Soeya, D. S. Kim, Sekiyu Gakkaishi, J. Jpn. Petrol. Inst. 33 (6) (1990) 347.
[11] R. B. Quincy, M. Houalla, A. Proctor, D. M. Hercules, J. Catal. 125 (1990) 214.
[12] J. Ramirez, R. Cuevas, L. Gasque, M. Vrinat, M. Breysse, Appl. Catal. 71 (1991) 351.
[13] D. S. Kim, K. Segawa, T. Soeya, I. E. Washs, J. Catal. 136 (1992) 539.
[14] D. S. Kim, I. E. Washs, K. Segawa, J. Catal. 146 (1994) 268.
[15] R. G. Leliveld, A. J. van Dillen, J. W. Geus, D. C. Koningsberger, J. Catal. 165 (1997) 184.
[16] S. K. Maity, M. S. Rana, S. K. Bej, J. Ancheyta-Juárez, G. Murali Dhar, T. S. R. Parasada Rao, Appl. Catal. A 205 (2001) 215.
[17] D. Wang, W. Qian, A. Ishihara, T. Kabe, J. Catal. 203 (2001) 322.
[18] D. Wang, W. Qian, A. Ishihara, T. Kabe, Appl. Catal. A 224 (2002) 191.
[19] E. Rodenas, T. Yamaguchi, H. Hattori, K. Tanabe, J. Catal. 69 (1981) 434.
[20] G. B. McVicker, J. -J. Ziemiak, J. Catal. 95 (1985) 473.
[21] K. Foger, J. R. Anderson, Appl. Catal. 23 (1986) 139.
[22] E. I. Ko, J. -P. Chen, J. G. Weissen, J. Catal. 105 (1987) 511.
[23] M. A. Stranick, M. Houalla, D. M. Hercules, J. Catal. 106 (1987) 362.
[24] A. Fernandez, J. Leyer, A. R. Gonzales-Elipe, G. Munuera, H. Knözinger, J. Catal. 112 (1988) 489.
[25] M. G. Reichmann, A. T. Bell, Appl. Catal. 32 (1987) 315.
[26] M. Anpo, T. Kawamura, S. Kodama, K. Maruya, T. Onishi, J. Phys. Chem. 92 (1988) 438.
[27] W. Zhaobin, X. Qin, G. Xiexian, E. L. Sham, P. Grange, B. Delmon, Appl. Catal. 63 (1990) 305.
[28] W. Zhaobin, X. Qin, G. Xiexian, E. L. Sham, P. Grange, B. Delmon, Appl. Catal. 75 (1991) 179.
[29] J. Ramirez, L. Ruiz-Ramirez, L. Cedeno, V. Harlé, M. Vrinat, M. Breysse, Appl. Catal. A 93 (1993) 163.
[30] H. M. Matralis, M. Ciardelli, M. Ruwet, P. Grange, J. Catal. 157 (1995) 368.
[31] B. M. Reddy, M. V. Kumar, E. P. Reddy, S. Mehdi, Catal. Lett. 36 (1996) 187.
[32] A. Guttiérez-Alejandro, M. Gonzales-Cruz, M. Trombetta, G. Busca, J. Ramirez, Micropor. Mesopor. Mater. 23 (1998) 265.
[33] E. Lecrenay, K. Sakanishi, T. Nagamatsu, I. Mochida, T. Suzuka, Appl. Catal. B 18 (3–4) (1998) 325.
[34] M. P. Borque, A. Lòpez-Agudo, E. Olguín, M. Vrinat, L. Cedeño, J. Ramirez, Appl. Catal. A 180 (1–2) (1999) 53.
[35] P. Concepción, B. M. Reddy, H. Knözinger, Phys. Chem. Chem. Phys. 1 (1999) 3031.
[36] V. Harlé, M. Vrinat, J. P. Scharff, B. Durand, J. P. Deloume, Appl. Catal. A 196 (2) (2000) 261.
[37] B. M. Reddy, B. Chowdury, E. P. Reddy, A. Fernández, Appl. Catal. A 213 (2001) 279.
[38] J. R. Grzechowiak, J. Rynkowski, I. Wereszczako-Zieliñska, Catal. Today 65 (2–4) (2001) 225.
[39] K. Segawa, M. Katsuta, F. Kameda, Catal. Today 29 (1996) 215.
[40] C. Pophal, F. Kameda, K. Hoshino, S. Yoshinaka, K. Segawa, Catal. Today 39 (1997) 21.
[41] S. Yoshinaka, K. Segawa, Catal. Today 45 (1998) 293.
[42] K. Segawa, K. Takahashi, S. Satoh, Catal. Today 63 (2000) 123.

[43] B.L. Shen, D.Y. Li, Y.L. Shen, PCT/CN 94/00087.
[44] S. Dzwigaj, C. Louis, M. Breysse, M. Cattenot, V. Bellière, C. Geantet, M. Vrinat, P. Blanchard, E. Payen, S. Inoue, H. Kudo, Y. Yoshimura, Appl. Catal. B 41 (2003) 181.
[45] D. Wang, W. Qian, A. Ishihara, T. Kabe, J. Catal. 209 (2002) 266.
[46] D. D. Whitehurst, T. Isoda, I. Mochida, Adv. Catal. 42 (1998) 345.
[47] R. Shafi, G. J. Hutchings, Catal. Today 59 (2000) 423.
[48] N. K. Nag, J. Phys. Chem. 91 (1987) 2324.
[49] Th. Weber, J. C. Muijsers, J. H. M. C. van Wolput, C. P. J. Verhagen, J. W. Niemantsverdriet, J. Phys. Chem. 100 (1996) 14144.
[50] C. P. Li, D. M. Hercules, J. Phys. Chem. 88 (1984) 456.
[51] M. Houalla, N. K. Nag, A. V. Sapre, D. H. Broederick, B. C. Gates, AIChE J. 24 (1978) 1015.
[52] R. Edvinsson, S. Irandoust, Ind. Eng. Chem. Res. 32 (1993) 391.
[53] G. F. Froment, G. A. Depauw, V. Vanrysselberghe, Ind. Eng. Chem. Res. 33 (1994) 2975.
[54] X. Ma, K. Sakanishi, T. Isoda, I. Mochida, Energy Fuels 9 (1995) 33.
[55] M. Houalla, D. H. Broederick, A. V. Sapre, N. K. Nag, V. H. J. D. Beer, J. Catal. 61 (1980) 523.
[56] G. H. Singhal, R. L. Espino, J. E. Sobel, G. A. Huff, J. Catal. 67 (1981) 457.
[57] V. Lamuremeille, E. Schulz, M. Lemaire, M. Vrinat, Appl. Catal. A 131 (1995) 143.
[58] V. Meille, E. Schulz, M. Lemaire, M. Vrinat, J. Catal. 170 (1997) 29.
[59] Q. Zhang, A. Ishihara, T. Kabe, J. Jpn. Petrol. Inst. 39 (1996) 410.
[60] D. R. Kilanowski, H. Teeuwen, B. C. Gates, V. H. J. D. Beer, G. C. A. Schuit, H. Kwart, J. Catal. 55 (1978) 129.
[61] M. V. Landau, D. Berger, M. Herskowitz, J. Catal. 158 (1996) 236.
[62] D. Yitzhaki, M. V. Landau, D. Berger, M. Herskowitz, Appl. Catal. A 122 (1995) 99.